

Piotr NIESLONY¹
Wit GRZESIK¹
Krzysztof ZAK¹
Piotr LASKOWSKI²

3D FEM SIMULATIONS AND EXPERIMENTAL STUDIES OF THE TURNING PROCESS OF INCONEL 718 SUPERALLOY

This paper is focused on the finite element analysis of machining of Inconel 718 superalloy in a non-orthogonal (3D) turning process. The cutting experiments were carried out on the cylindrical workpiece of Inconel 718 with the cutting speed of 60-90 m/min, the feed rate of 0.1 mm/rev and different depths of cut. The FEM simulations include the average and maximum interface temperatures, the resultant cutting force and its three components and the chip thickness obtained for the 3D turning process. The simulation results were compared with experimental data obtained in the non-orthogonal process. It was found that the experimental values of the cutting forces are underestimated (about 23-30%) in relation to the FEM simulation data. Additionally, it was noted that the cutting depth has a significant effect on the average interface temperature only when using a non-orthogonal turning process.

1. INTRODUCTION

Inconel 718 is a high strength, thermal resistant nickel-based superalloy. It is known to be one of the most difficult-to-machine materials because of its high hardness, high strength at high temperatures and low thermal conductivity. The assessment of machinability of the superalloys has been a topic of research over the last years. It is observed that most of the efforts are directed towards assessing the life of cutting tools and disclosing tool wear mechanisms in machining of this nickel-based superalloy [1],[2],[3]. Besides that, the cutting force during machining of Inconel 718 has been investigated by some authors [4],[5]. It should be noted that the majority of publications concern the modeling of superalloy machining during orthogonal cutting tests.

Recently, more and more researchers have presented their finite element simulations in the machining of this alloy. The Johnson-Cook (J-C) model is still the most popular model

¹ Opole University of Technology, Faculty of Mechanical Engineering, Poland, E-mail: p.nieslony@po.opole.pl

² Rzeszow University of Technology, Poland

for the machining simulation due to its robustness and ease of application in the FE codes [6],[7]. But some researchers [5],[8] use other constitutive models in the FEM simulation. In this case study, a Power Law model is used together with the J-C law.

One of the aims of FEM simulation tests is to produce an efficient numerical model for the prediction of the thermal and mechanical characteristics of machining and other manufacturing processes [9].

It is well known that the numerical models need to be validated with a reliable experimental database. This paper presents a finite element model for the turning of Inconel 718 using the original 3D CAD model of the grooved cutting insert. The effects of the cutting speed and cutting depth on cutting forces and the cutting temperature in a non-orthogonal turning process of Inconel 718 are investigated.

2. METHODOLOGY OF INVESTIGATIONS

In this study, non-orthogonal turning trials were carried out on a CNC lathe equipped with a Kistler9257B piezoelectric dynamometer with a 5019B amplifier and NI 6062E, National Instruments, A/D multi-channel board. The visualization of the recorded force signals and their processing was performed using CutPro data acquisition system. The experimental and simulation conditions are specified in Table 1.

Table 1. Configurations of experimental and numerical simulations

Cutting condition	$v_c=60 \div 90\text{m/min}$, $a_p=0.125, 0.250, 1.0$ and 2.0mm , $f=0.1\text{mm/rev}$
Tool data	Grooved tool (KM) type CNMG 120412-UP Sintered carbide insert H10 coated with TiAlN layer of $3\mu\text{m}$ thick Cutting edge radius $r_n=50\mu\text{m}$
Tool geometry	Cutting tool angles: orthogonal rake $\gamma_o=-5^\circ$, orthogonal clearance $\alpha_o=5^\circ$, back rake $\gamma_p=-4.55^\circ$, side rake $\gamma_f=-5.41^\circ$, tool inclination angle $\lambda_s=-5.0^\circ$ Tool nose radius $r_\epsilon=1.2\text{mm}$
Simulation models	Three dimensional (3D)

The experiments and FEM simulations were performed for cutting inserts with grooved rake faces. In this case CNMG 120412-UP cutting tool inserts coated with a TiAlN monolayer produced by Kennametal were used [10]. The measured value of the cutting edge

radius for this insert was equal to $r_n=50\mu\text{m}$. The finite element modeling was performed in AdvantEdge package. For the FEM simulation the original 3D CAD model of the grooved cutting insert was used. The dimensioned groove and the cutting edge along with the magnified corner area are presented in Fig. 1.

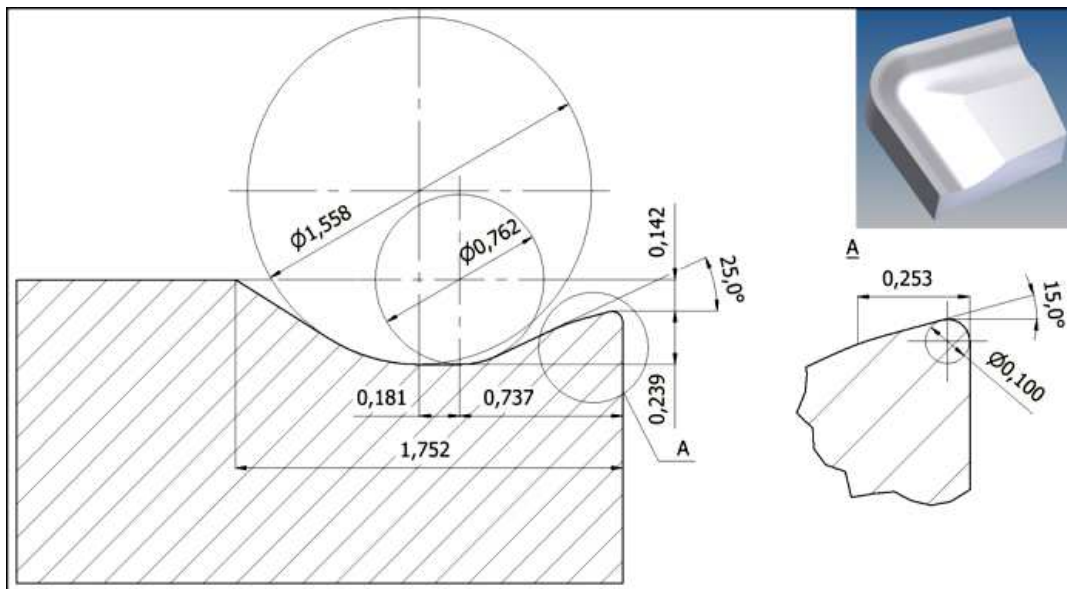


Fig. 1. Dimensioned cross-section of CNMG 120412-UP cutting insert with CAD model of the tool wedge used in FEM simulation

3. EXPERIMENTAL RESULTS

3.1. THERMAL EFFECTS

The analysis of the experimental results was performed in two stages. The first part was focused on the variations of the average cutting temperature resulting from the variations of process parameters for non-orthogonal (3D) FEM simulations. The second stage concerns the assessment of the influences of the process parameters and FEM predictions on the maximum value of the cutting temperature.

It can be observed in Fig. 2 that the dynamic signal of temperature at the tool-chip interface was generated. Its processing allows both average (t_{ave}) and maximum (t_{max}) values of the temperature to be determined. An example of the signal analysis in the form of the window is presented in Fig. 2.

Fig. 3 presents the changes of the average (Fig. 3a) and maximum (Fig. 3b) interface temperatures resulting from variations of the cutting speed and the depth of cut. The feed rate was kept constant at 0.1mm/rev. Moreover, the values of the depth of cut were selected for medium ($a_p=1$ and 2mm) as well as for finish turning ($a_p=0.125$ and 0.25mm).

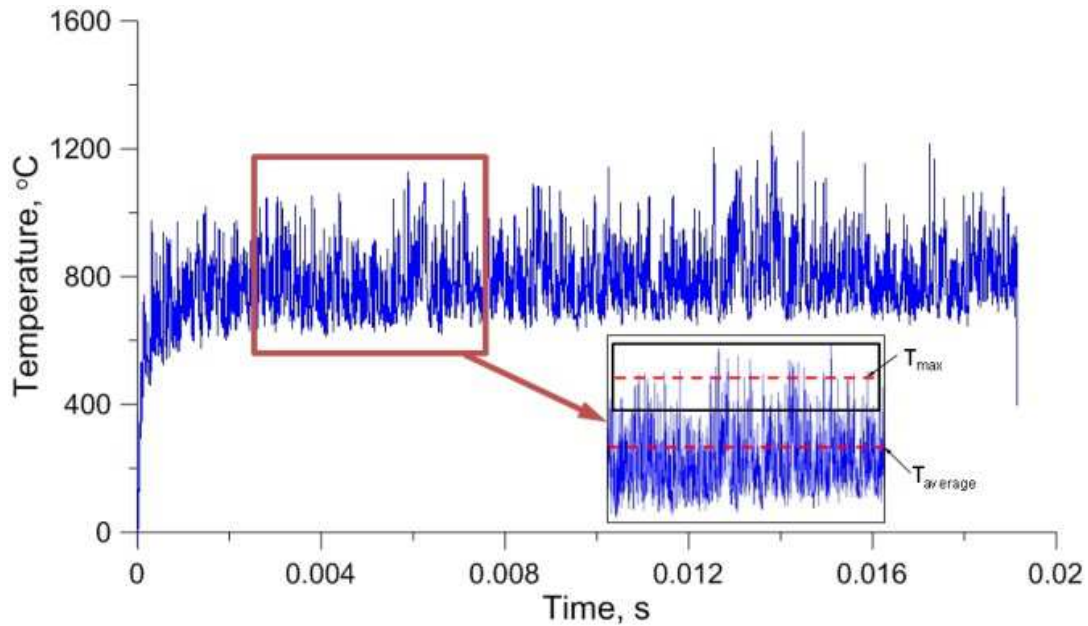


Fig. 2. Signal waveform of cutting temperature vs. time with defined zoomed area of average and maximum temperatures. Cutting parameters: $v_c=60\text{m/min}$, $f=0.1\text{mm/rev}$, $a_p=1\text{mm}$

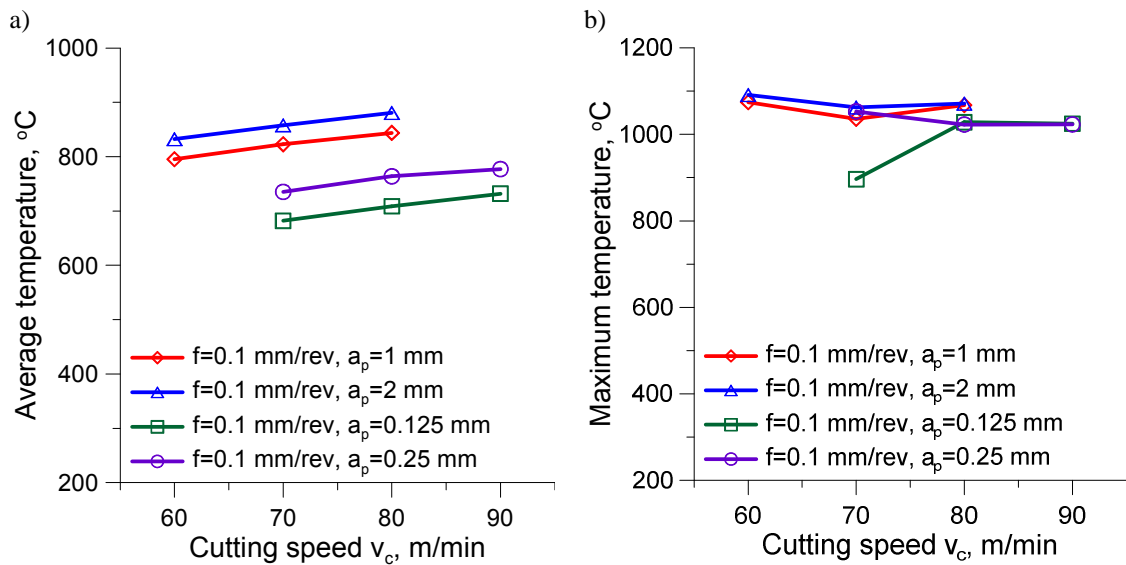


Fig. 3. Comparison of the average (a) and maximum (b) temperatures for 3D FEM simulation models

It was observed in Fig. 3a that the increase of the depth of cut causes that the average temperature increases slightly. For the two values of a_p used (0.125 and 2.0mm) and the cutting speed of 80 m/min the values of the average temperature differs by about 200°C. This fact suggests that the choice of the depth of cut in the turning of Inconel 718 seems to be important in terms of the cutting temperature. According to Fig. 3a, the influence of the cutting speed is visible and the percentage changes are in the range of 7-12%.

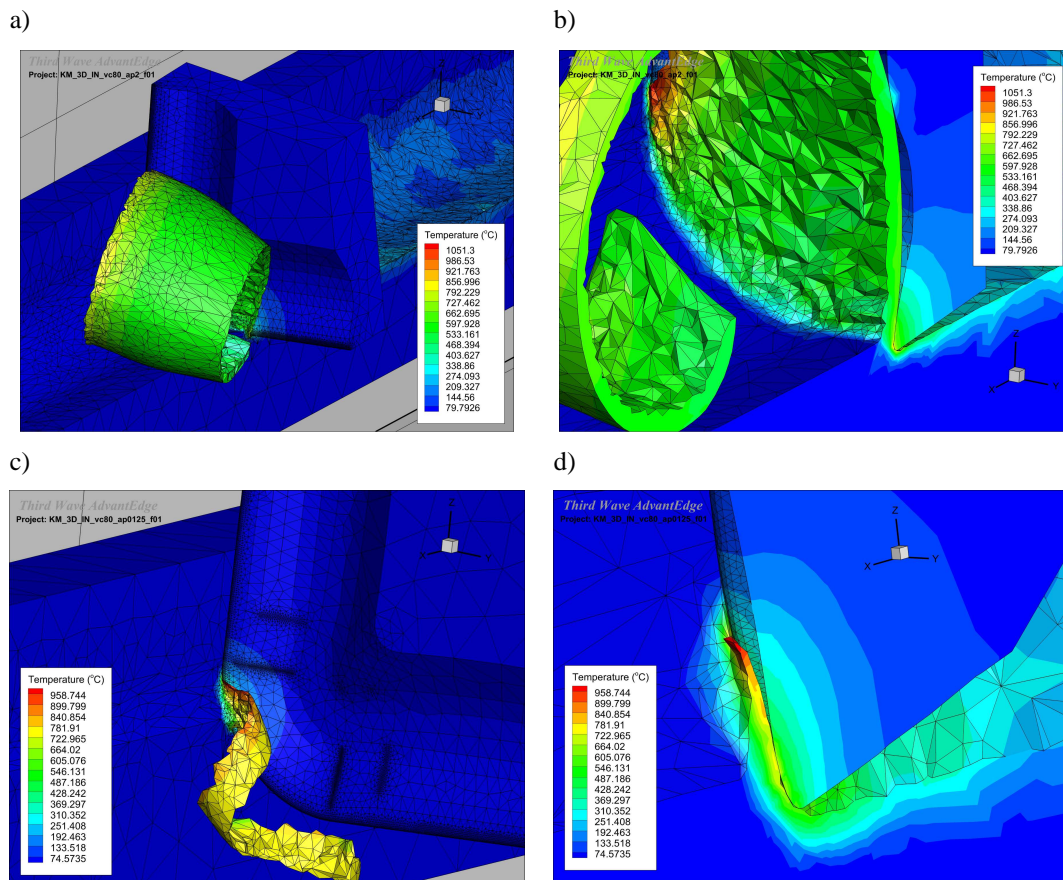


Fig. 4. Visualization of the FEM simulation results (a,c) with slice images of the cutting zone (b,d). Process parameters: $v_c=80\text{m/min}$, $f=0.1\text{mm/rev}$, $a_p=2\text{mm}$ (a,b) and 0.125mm (c,d)

On the other hand, the changes of the maximum interface temperature t_{\max} are presented in Fig. 3b. In this case, the influence of the depth of cut on the maximum interface temperature can be ignored. However, the difference between the maximum and average values of the interface temperature resulting from the variation of the depth of cut ranges from $50\text{--}200^\circ\text{C}$. In 3D cutting simulations one can visualize the heat transfer in the cutting zone. For instance, Fig. 4 shows exemplary images using the slice technique for the cutting speed of 80m/min and the lowest (0.125mm) and highest (2 mm) values of the depth of cut.

3.2. MECHANICAL EFFECTS

The measured and predicted values of the three componential forces F_c , F_f and F_p are specified in Fig. 5. This comparison was based on the well known fact that the depth of cut predominantly influences the cutting forces. The general conclusion is that a 3D simulation allows to differentiate between the three components of the resultant cutting force. For the highest depth of cut of 2mm (Fig. 5a) a higher cutting force F_c and a lower passive force F_p

were determined. When the dept of cut is decreased to 1mm the passive force decreases and the values of the feed and passive forces are comparable to each other. In contrast, for finish turning with substantially lower depths of cut of 0.125mm and 0.250mm, comparable values of the cutting and passive forces were determined, as shown in Fig. 5b.

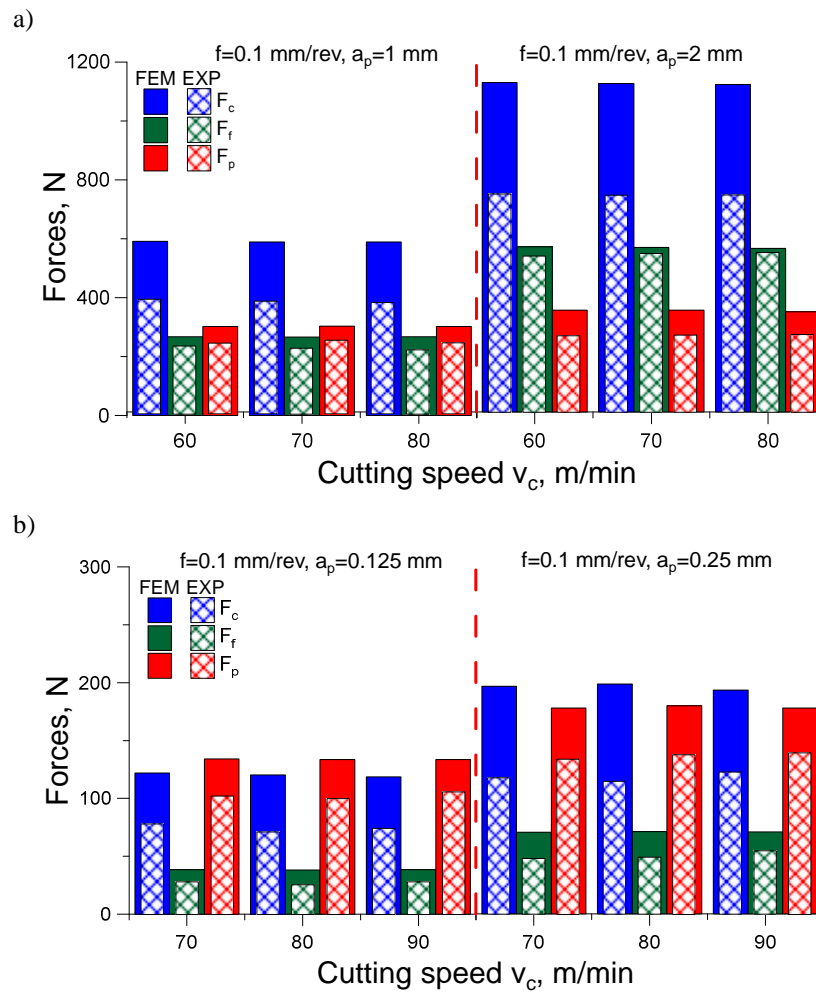


Fig. 5. Comparison of the components of resultant cutting force obtained with experimental tests and FEM simulations in non-orthogonal turning processes for lower (a) and higher (b) values of depth of cut

The different relationships between componential forces result from the fact that for low depths of cut the tool nose takes part in the machining. It should be noted that for the tool nose radius of $r_e=1.2$ mm and $a_p=1$ mm the active part of the cutting edge is only curvilinear [11]. Fig. 5 also presents the comparison between measured and simulated (predicted) values of the three force components. In general, a better fitting of the predictions to the measurements is observed for the feed F_f and passive F_p forces and for these two cases the differences are of about 7-13%. On the other hand, they are higher of about 30% for the cutting force F_c .

For smaller depths of cut the prediction errors are higher. They are about 40% for the cutting F_c and feed F_f forces and about 20% for the passive force. It should be noted in Fig. 5b that the participation of the componential forces corresponds to the measured data. As mentioned earlier, the decrease of the depth of cut results in the increase of the passive force and the decrease of the feed force.

The comparison of the mechanical loads exerted on the cutting tool is extended to the resultant cutting force as shown in Fig. 6. As shown in Fig. 6 the influence of the cutting speed in the range of 60-90m/min on the resultant cutting force can be neglected. The prediction errors for the depth of cut equal to 2mm is on average of about 23%. For smaller depths of cut the prediction are less accurate and the appropriate errors increase to 28%.

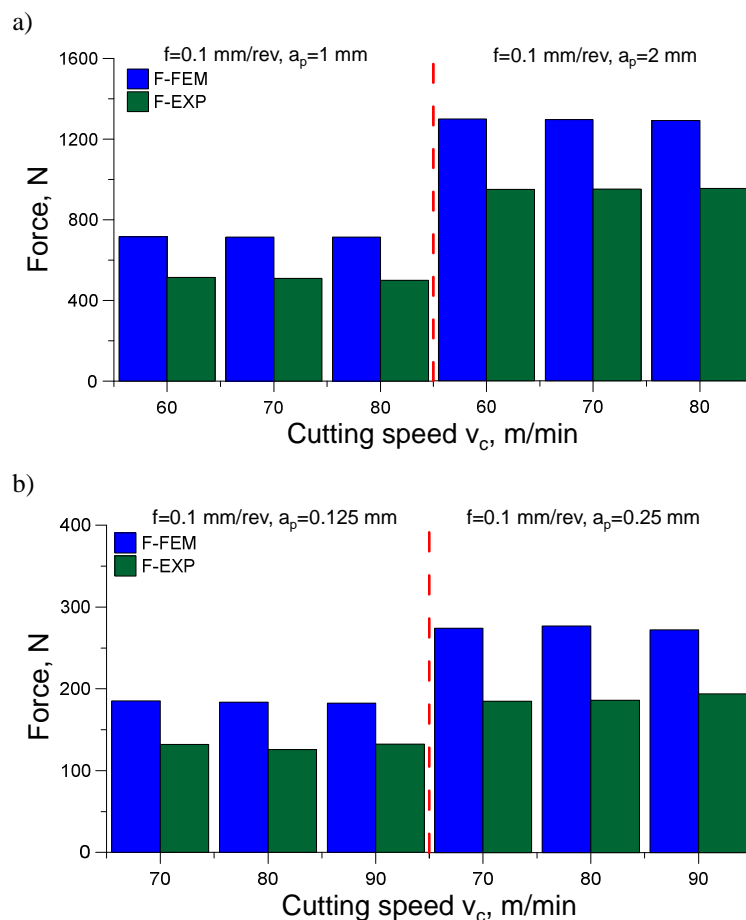


Fig. 6. Quantitative comparison of the measurements and semi-orthogonal FEM simulations of the resultant cutting force obtained for higher: (a) and lower (b) values of depth of cuts and different cutting speeds

Such distinct prediction errors originate from the difficulties in the accurate meshing of the cutting zone. In the case when the tool nose predominantly takes part in the metal removal, some problems appear with meshing and re-meshing in the cutting zone. As a result, they generate considerable errors in the FEM predictions.

3.3. PLASTIC DEFORMATION

As show in Fig. 4a the spirally curled chip is generated during 3D simulations. The chip form depends on the machining parameters used and the geometry of the chip breaking groove on the rake face. After simulations both the undeformed chip thickness h and the chip thickness h_{ch} were measured using a special graphical program Tecplot integrated with the FEM package AdvantEdge [12], as shown in Fig. 7. Because the chip thickness is not uniform, the maximum and minimum values were determined and the average values were computed. All obtained data are specified in Table 2. As a result, the chip compression ratio λ_h was determined as the ratio of the chip thickness h_{ch} to the undeformed chip thickness h (eqn.1).

$$\lambda_h = \frac{h_{ch}}{h} \quad (1)$$

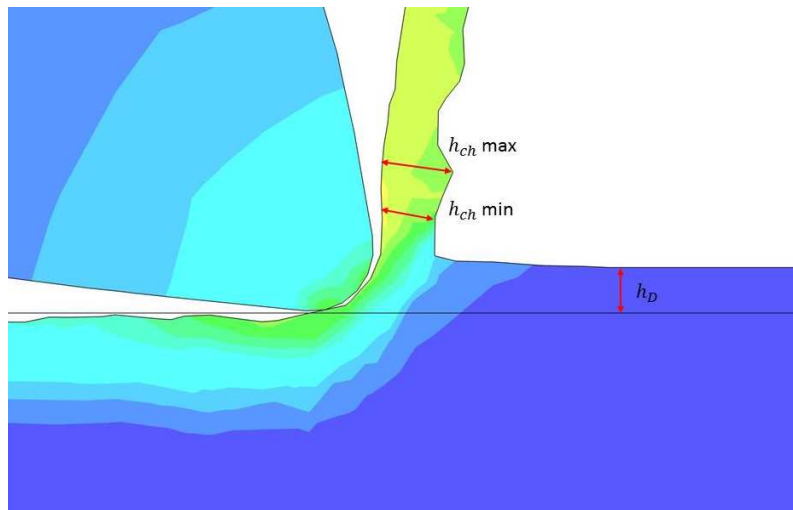


Fig. 7. Determination of the cut layer h and chip thickness h_{ch} in AdvantEdge Tecplot360 for $v_c=80\text{m/min}$, $f=0.1\text{mm/rev}$ and $a_p=0.125\text{mm}$

Table 2. Values of chip thickness and the real undeformed chip thickness obtained from FEM simulation

a_p, mm	$f, \text{mm/rev}$	h, mm	h_{ch}, mm		$h_{ch} \text{ average}, \text{mm}$
			<i>min</i>	<i>max</i>	
0.125	0.05	0.020	0.027	0.032	0.030
	0.10	0.043	0.042	0.06	0.052
0.25	0.05	0.026	0.034	0.046	0.041
	0.10	0.060	0.073	0.083	0.079
1.0	0.10	0.070	0.115	0.124	0.119
	0.15	0.140	0.180	0.218	0.200
2.0	0.10	0.090	0.114	0.149	0.134
	0.15	0.150	0.189	0.206	0.197

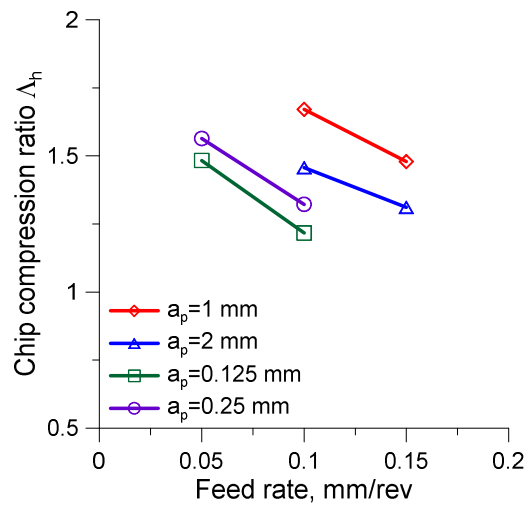


Fig. 8. Chip compression ratio vs. feed rate appointed from the 3D simulation for constant cutting speed $v_c=80\text{m/min}$ and different depth of cuts

It should be noted that the chip compression ratio is a quantitative measure of the degree of the plastic deformation occurring in the cutting zone. It represents the true strain in the plastic deformation and can be used to calculate the elementary work spent over plastic deformation of a unit volume of the work material [11],[13]. The influence of the feed rate and the depth of cut on the chip compression ratio (CCR) is presented in Fig. 8. As shown in Fig. 8 the chip deformation depends on both these technological parameters but more intensively on the feed rate used. In general, the lower the feed rate, the higher plastic deformation of the chip. This fact can be explained in terms of a greater strain-hardening effect occurring at a lower feed (thinner unreformed chip removed) and the associated size effect [11]. Moreover, a smaller feed rate concerns the higher specific cutting pressure. In Fig. 8, two groups of graphs for smaller and larger depths of cut are distinguished. The predicted values of the CCR are compared with the experimental data provided by Thakura et al. [14] and Hagberg and Malm [15]. Quite a good agreement was reached when comparing these results.

4. SUMMARY

Based on the experimental results and FEM predictions the conclusions are as follows:

- The analysis of the 3D FEM simulations using special graphical programs is capable of accurately determining the mechanical and thermal loads as well as the plastic deformation in the cutting zone.
- During machining of Inconel 718 the average interface temperature depends on the depth of cut. Lower temperatures were predicted for finish machining with a smaller depth of cuts. On the other hand, the maximum interface temperature is, in general,

independent of the depth of cut applied. However, its value is important in terms of the thermal regime of the coated cutting inserts.

- A comparison of the predicted and measured components of the resultant cutting force indicates that the FEM predictions exceed experimental values. The prediction errors are somewhat lower for medium machining but in general they exceed 20%. The highest errors are determined for the cutting force F_c .
- Higher values of the passive force F_p were predicted when machining with smaller depths of cut. This fact suggests the predominant role of the tool nose in generating the machined surface.
- The chip deformation depends on the feed rate and the depth of cut used. Machining with the smallest feed rates causes the strain-hardening effect increase and the size effect occurs.

ACKNOWLEDGEMENTS

This investigations have been carried out as part of the project No. PBS1-178595 funded by the Polish National Center for Research and Development (NCBiR).

REFERENCES

- [1] COSTES J.P., GUILLET Y., POULACHON G., et al., 2007, *Tool-life and wear mechanisms of CBN tools in machining of Inconel 718*, Int. J. Mach. Tools Manuf., 47, 1081–1087.
- [2] ALTIN A., NALBANT M., TASK A., 2007, *The effects of cutting speed on tool wear and tool life when machining Inconel 718 with ceramic tools*, Materials and Design, 28, 2518–2522.
- [3] DEVILLEZ A., SCHNEIDER F., DOMINIAK S., DUDZINSKI D., LARROQUERE D., 2007, *Cutting forces and wear in dry machining of Inconel 718 with coated carbide tools*, Wear, 262, 931–942.
- [4] PAWADEA R.S., JOSHA SUHAS S., BRAHMANKAR P.K., 2008, *Effect of machining parameters and cutting edge geometry on surface integrity of high-speed turned Inconel 718*, Int. J. Mach. Tools Manuf., 48, 15–28.
- [5] ZHENCHAO Y., DINGHUA Z., XINCHUN H., CHANGFENG Y., YONGSHOU L., YING M., 2011, *The simulation of cutting force and temperature field in turning of Inconel 718*, Key Engineering Materials, 458, 149–154.
- [6] MUTHU E., SENTHAMARAI K., JAYABAL S., 2012, *Finite element simulation in machining of Inconel 718 nickel based superalloy*, Int. J of Adv. Eng. Applic., 1/3, 22-27.
- [7] NIESLONY P., GRZESIK W., 2013, *Sensitivity analysis of the constitutive models in FEM-based simulation of the cutting process*, Journal of Machine Engineering, 13/1, 106-116.
- [8] NIESLONY P., GRZESIK W., CHUDY R., LASKOWSKI P., HABRAT W., 2013, *3D FEM simulation of titanium machining*, International Conference on Advanced Manufacturing Engineering and Technologies – NEWTECH, 31-40.
- [9] BERRUTI T., LAVELLA M., GOLA M. M., 2009, *Residual stresses on Inconel 718 turbine shaft samples after turning*, Mach. Sci. Technol., 13/4, 543-560.
- [10] KENNAMETAL, 2013, May 15. Available: <http://www.kennametal.com>.
- [11] GRZESIK W., 2008, *Advanced machining processes of metallic materials: Theory, Modelling and Applications*, Elsevier, Amsterdam.
- [12] THIRD WAVE ADVANTEDGE, 2011, User's Manual-Version 5.8, Minneapolis, USA.

- [13] MATIVENGA P.T., ABUKHSHIM N.A., SHEIKH M.A., HON B.K.K., 2006, *An investigation of tool chip contact phenomena in high-speed turning using coated tools*, Proceedings of the Institution of Mechanical Engineers. Part B. 220, 657–667.
- [14] THAKUR D.G., RAMAMOORTHY B., VIJAYARAGHAVAN L., 2009, *Machinability investigation of Inconel 718 in high-speed turning*, Int. J. Adv. Manuf. Technol., 45, 421–429.
- [15] HAGBERG A., MALM P., 2010, *Material deformation mechanisms during machining of superalloys*, Diploma work, 28, Chalmers University of Technology, Gothenburg, Sweden.